

Nonlinear dynamics induced by parallel and orthogonal optical injection in 1550 nm Vertical-Cavity Surface-Emitting Lasers (VCSELs)

Antonio Hurtado,^{1,*} Ana Quirce,^{2,3} Angel Valle,² Luis Pesquera,² and Michael J. Adams¹

¹*School of Computer Science and Electronic Engineering, University of Essex, Wivenhoe Park, CO4 3SQ, Colchester, UK.*

²*Instituto de Física de Cantabria (CSIC-Univ. Cantabria), Avda. Los Castros s/n, E39005, Santander, Spain*

³*Dept. de Física Moderna, Fac. Ciencias, Univ. Cantabria, Avda. Los Castros s/n, E39005, Santander, Spain*
*ahurt@essex.ac.uk

Abstract: We report a first experimental study of the nonlinear dynamics appearing in a 1550 nm single-mode VCSEL subject to parallel and to orthogonal optical injection. For the first time to our knowledge we report experimentally measured stability maps identifying the boundaries between regions of different nonlinear dynamics for both cases of polarized injection. A rich variety of nonlinear behaviours, including periodic (limit cycle, period doubling) and chaotic dynamics have been experimentally observed.

©2010 Optical Society of America

OCIS codes: (140.7260) Vertical cavity surface emitting lasers; (190.3100) Instabilities and chaos; (230.5440) Polarization-selective devices; (130.4815) Optical switching devices.

References and links

1. F. Koyama, "Recent advances of VCSEL photonics," *IEEE J. Lightwave Technol.* **24**(12), 4502–4513 (2006).
2. R. Lang, "Injection locking properties of semiconductor laser," *IEEE J. Quantum Electron.* **18**(6), 976–983 (1982).
3. T. B. Simpson, J. M. Liu, and A. Gavrielides, "Bandwidth enhancement and broadband noise reduction in injection-locked semiconductor lasers," *IEEE Photon. Technol. Lett.* **7**(7), 709–711 (1995).
4. X. Meng, T. Chau, and M. C. Wu, "Experimental demonstration of modulation bandwidth enhancement in distributed feedback lasers with external light injection," *Electron. Lett.* **34**(21), 2031–2032 (1998).
5. C.-H. Hang, L. Chrostowski, and C. J. Chang-Hasnain, "Injection locking of VCSELs," *IEEE J. Sel. Top. Quantum Electron.* **9**(5), 1386–1393 (2003).
6. L. Chrostowski, B. Faraji, W. Hofmann, M.-C. Amann, S. Wiczorek, and W. W. Chow, "40 GHz bandwidth and 64 GHz resonance frequency in injection-locked 1.55 μm VCSELs," *IEEE J. Sel. Top. Quantum Electron.* **13**(5), 1200–1208 (2007).
7. Q. Gu, W. Hoffmann, M.-C. Amann, and L. Chrostowski, "Optically injection-locked VCSEL as a duplex transmitter/receiver," *IEEE Photon. Technol. Lett.* **20**(7), 463–465 (2008).
8. Z. G. Pan, S. Jiang, M. Dagenais, R. A. Morgan, K. Kojima, M. T. Asom, R. E. Leibenguth, G. D. Guth, and M. W. Focht, "Optical injection induced polarization bistability in vertical-cavity surface-emitting lasers," *Appl. Phys. Lett.* **63**(22), 2999–3001 (1993).
9. I. Gatara, J. Buesa, H. Thienpont, K. Panajotov, and M. Sciamanna, "Polarization switching bistability and dynamics in vertical-cavity surface-emitting laser under orthogonal optical injection," *Opt. Quantum Electron.* **38**(4-6), 429–443 (2006).
10. K. H. Jeong, K. H. Kim, S. H. Lee, M. H. Lee, B. S. Yoo, and K. A. Shore, "Optical injection-induced polarization switching dynamics in 1.5 μm wavelength single-mode vertical-cavity surface-emitting lasers," *IEEE Photon. Technol. Lett.* **20**(10), 779–781 (2008).
11. A. Hurtado, I. D. Henning, and M. J. Adams, "Two-wavelength switching with a 1550nm VCSEL under single orthogonal optical injection," *IEEE J. Sel. Top. Quantum Electron.* **14**(3), 911–917 (2008).
12. A. Quirce, A. Valle, and L. Pesquera, "Very wide hysteresis cycles in 1550 nm-VCSELs subject to orthogonal optical injection," *IEEE Photon. Technol. Lett.* **21**(17), 1193–1195 (2009).
13. A. Valle, M. Gomez-Molina, and L. Pesquera, "Polarization bistability in 1550nm wavelength single-mode vertical-cavity surface-emitting lasers subject to orthogonal optical injection," *IEEE J. Sel. Top. Quantum Electron.* **14**(3), 895–902 (2008).
14. A. Hurtado, I. D. Henning, and M. J. Adams, "Different forms of wavelength polarization switching and bistability in a 1.55 microm vertical-cavity surface-emitting laser under orthogonally polarized optical injection," *Opt. Lett.* **34**(3), 365–367 (2009).
15. Y. Hong, P. S. Spencer, P. Rees, and K. A. Shore, "Optical injection dynamics of two-mode vertical cavity surface-emitting semiconductor lasers," *IEEE J. Quantum Electron.* **38**(3), 274–278 (2002).

16. A. Homayounfar, and M. J. Adams, "Locking bandwidth and birefringence effects for polarized optical injection in vertical-cavity surface-emitting lasers," *Opt. Commun.* **269**(1), 119–127 (2007).
17. I. Gatare, M. Sciamanna, M. Nizette, H. Thienpont, and K. Panajotov, "Mapping of two-polarization-mode dynamics in vertical-cavity surface-emitting lasers with optical injection," *Phys. Rev. E Stat. Nonlin. Soft Matter Phys.* **80**(2), 026218 (2009).
18. M. Sciamanna, and K. Panajotov, "Route to polarization switching induced by optical injection in vertical cavity surface-emitting lasers," *Phys. Rev. A* **73**(2), 023811 (2006).
19. J. Buesa, I. Gatare, K. Panajotov, H. Thienpont, and M. Sciamanna, "Mapping of the dynamics induced by orthogonal optical injection in vertical-cavity surface-emitting lasers," *IEEE J. Quantum Electron.* **42**(2), 198–207 (2006).
20. K. Panajotov, I. Gatare, A. Valle, H. Thienpont, and M. Sciamanna, "Polarization- and Transverse-Mode Dynamics in Optically Injected and Gain-Switched Vertical-Cavity Surface-Emitting Lasers", in *IEEE J. Quantum Electron.* **45**(11), 1473–1481 (2009).
21. A. Hurtado, I. D. Henning, and M. J. Adams, "Differences in the injection locking bandwidth in 1550nm-VCSELs subject to parallel and orthogonal optical injection", *IEEE 21st International Semiconductor Laser Conference, 2008, ISLC 2008*, 87–88, Sorrento (Italy), 14–18 September 2008.
22. A. Quirce, A. Hurtado, A. Valle, L. Pesquera, and M. J. Adams, "Nonlinear Polarization Dynamics Induced by Orthogonal Optical Injection in 1550nm Vertical-Cavity Surface-Emitting Lasers", *22nd Annual Meeting of the IEEE Photonics Society, PHO 2009, Belek-Antalya (Turkey)*, 4–9 October 2009.
23. F. Mogensen, H. Olesen, and G. Jacobsen, "Locking conditions and stability properties for a semiconductor laser with external light injection," *IEEE J. Quantum Electron.* **21**(7), 784–793 (1985).
24. S. Wieczorek, B. Krauskopf, T. B. Simpson, and D. Lenstra, "The dynamical complexity of optically injected semiconductor lasers," *Phys. Rep.* **416**(1-2), 1–128 (2005).
25. M.-R. Park, "O.-Kyun Kwon, W.-S. Han, K.-H. Lee, S.-J. Park and B.-S. Yoo, "All-monolithic 1.55µm InAlGaAs/InP vertical cavity surface emitting lasers grown by metal organic chemical vapor deposition," *Jpn. J. Appl. Phys.* **45**, L8–L10 (2006).

1. Introduction

Long-wavelength Vertical-Cavity Surface Emitting Lasers (VCSELs) emitting at the telecom wavelength of 1550 nm are very promising devices as they offer inherent advantages in comparison to edge-emitting devices. These advantages include, reduced fabrication costs, high coupling efficiency to optical fibres, on-wafer testing capability, ease of fabrication of 2D arrays, single-mode operation, low-threshold current, compactness, etc [1]. Additionally, optical injection locking is a well known technique to improve the performance of semiconductor lasers without modifying the laser design [2–4]. Recently, reduced chirp, reduced nonlinearities and enhanced modulation bandwidth [5–7] have been reported in injection-locked 1550nm-VCSELs, making these devices ideal candidates for use as stable sources in present and future optical telecommunication networks.

Additionally, the effect of polarized optical injection in VCSELs has attracted increasing interest in the last years [8–21]. In particular, orthogonally-polarized optical injection has been used to obtain Polarization Switching (PS) and Polarization Bistability (PB) in short- [8] [9] and in long-wavelength VCSELs [10–14]. Single mode operation has been attained in multiple transverse mode VCSELs [15] under orthogonal optical injection. Also a wide variety of nonlinear dynamics has been recently theoretically [16–18] and experimentally [19] [20] reported in VCSELs subject to orthogonal injection. However, the effect of polarized injection on the stability analysis of optically-injected VCSELs has received little attention. An experimental stability map has been reported for an 845 nm-VCSEL subject to orthogonally-polarized optical injection, identifying the boundaries between regions of stable locking, unlocking, bistability and chaos [19]. Recently, we have focused on the stability analysis of 1550 nm-VCSELs subject to different polarized optical injection and we have reported the first injection locking diagrams for these devices subject to parallel and orthogonal optical injection [21] as well as a first preliminary analysis of the nonlinear dynamics appearing under orthogonal optical injection [22].

In this work we report for the first time to our knowledge an experimental study of the nonlinear dynamics of a 1550 nm-VCSEL subject to parallel and to orthogonal optical injection. In contrast with previous experiments with 845nm-VCSELs [19] our device is single transverse mode with a preferred polarization. Moreover the frequency of the parallel polarization is higher than that of the orthogonal one with a much larger frequency difference between both polarizations. For both cases of polarized injection we have measured stability

maps identifying the boundaries between regions of different behaviour, including periodic dynamics (such as limit cycle and period doubling), chaos and polarization switching (PS). Our results show a difference in the shape of the stability maps depending on the polarization of optical injection. For the case of parallel polarization similar results to those reported in edge-emitting devices [23] [24] are found. On the other hand, a different shape with new qualitative features with respect to previous results [19] is reported for the measured stability map when the 1550 nm-VCSEL is subject to orthogonal optical injection.

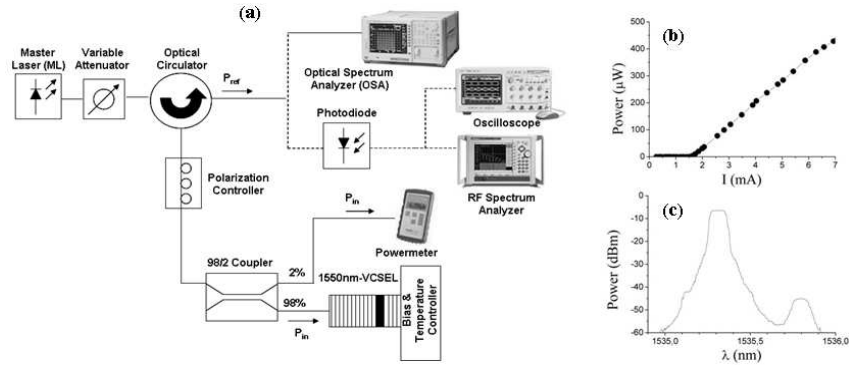


Fig. 1. (a) Experimental setup. (b) L-I curve and (c) spectrum of the VCSEL.

2. Experimental Setup

Figure 1(a) shows the all-fibre setup that has been developed to inject the light emitted by a tuneable laser (Master Laser, ML) into the 1550 nm-VCSEL (Slave Laser, SL). A variable optical attenuator is included after the ML to control the level of optical power of the externally injected signal. The output of the ML is then injected into the SL using an optical circulator. The polarization of the external signal is controlled using a fibre polarization controller. A 98/2 fibre directional coupler divides the optical path in two branches; the 2% branch is used to monitor the optical input power with a power meter whereas the 98% output is directly connected to the SL. Finally, the reflected output of the SL was analyzed by connecting different measurement equipment to the third port of the circulator. The stability of the reflected signal was analyzed optically with an Optical Spectrum Analyzer (OSA), and electrically with an Electrical Spectrum Analyzer (RF Analyzer) and also with an Oscilloscope for the measurement of time traces. A fast-photodiode (9 GHz bandwidth) was used to transform the optical signal to the electrical domain.

A commercially available quantum-well 1550 nm-VCSEL (Raycan) [25] was used in the experiments. Figure 1(b) plots the L-I curve of the device measured at a temperature of 298 K, showing a threshold current (I_{th}) of 1.64 mA. Figure 1(c) shows the optical spectrum of the VCSEL biased at 6.0 mA (also at 298 K). The two modes in Fig. 1(c) correspond to the two orthogonal polarizations of the fundamental transverse mode of the device. The lasing mode has “parallel” polarization and appears at the wavelength $\lambda_{||} = 1535.3$ nm whereas the subsidiary mode has “orthogonal” polarization and its wavelength (λ_{\perp}) is shifted 0.49 nm to the long-wavelength side of the lasing mode. This value for the frequency splitting between the two orthogonal polarizations is very large in comparison to those reported in short-wavelength devices [9]. Similar values of approximately 0.5 nm have been measured for various devices from the same manufacturer [10–14]. This large value of frequency splitting allowed us to clearly distinguish both modes in the optical spectrum and also permitted to perform the stability analyses independently for both cases of polarized optical injection without including polarization selective devices in the setup. A Side Mode Suppression Ratio (SMSR) of 38.7 dB was measured for the orthogonal polarization. Spectra of this form were measured for all biases and no polarization switching was observed for any applied bias above threshold. For more information about the VCSEL’s structure see [25].

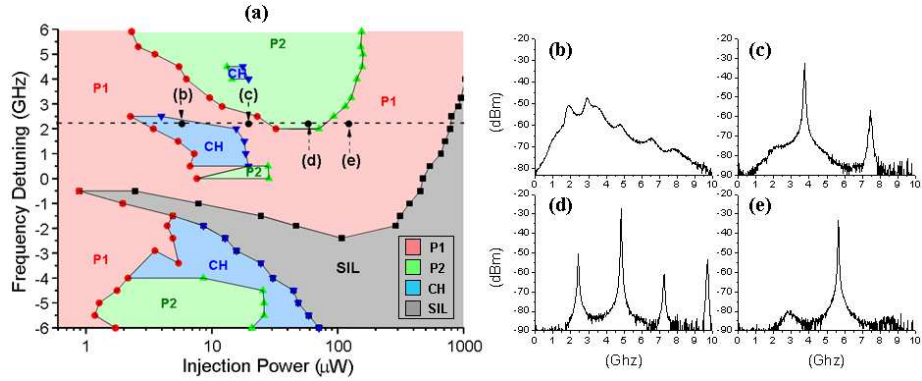


Fig. 2. (a) Experimental stability map of the 1550nm-VCSEL subject to parallel polarized injection; Different regions are observed: SIL (stable injection locking), P1 (Period 1), P2 (period 2) and CH (chaos); (b-e) RF spectra measured for the situations indicated in the stability map corresponding to a frequency detuning of 2.2 GHz and various levels of input power: (b) 5.8 μ W (chaos, CH), (c) 19.6 μ W (Period 1, P1), (d) 58.31 μ W (Period 2, P2) and (e) 122.5 μ W (Period 1, P1). Applied bias current of 4 mA ($I_{Bias} = 2.44 \times I_{th}$).

3. Experimental results

3.1 Parallel polarized optical injection

In studies of injection locking and nonlinear dynamics in semiconductor lasers, the polarization of the ML has been traditionally chosen to match that of the light emitted by the SL. Therefore, initially we have analyzed the case of parallel polarized injection into the parallel polarized lasing mode of the 1550 nm-VCSEL and Fig. 2(a) shows the experimental stability map for this case measured with the device biased with an applied current of 4 mA ($I_{Bias} = 2.44 \times I_{th}$). The frequency of the externally injected signal, f , was swept around the resonant frequency of the parallel polarization mode, $f_{||}$, the frequency detuning being $f - f_{||}$. Regions of different behaviour were observed, including periodic dynamics such as limit cycle (period 1, P1) and period doubling (period 2, P2) and regions of chaos. The latter were observed for both positive and negative frequency detuning. It is important to note here that the measured stability map exhibits strong similarities with those reported in edge-emitting devices (see [24] and references therein for a review). We believe that these similarities appear since we are matching the polarization of the external signal to that of the lasing mode. This conforms to the convention with edge-emitting lasers, where the polarizations of the ML and the SL are matched.

Figures 2(b-e) show the experimental RF spectra for the points marked in Fig. 2(a). Figure 2(b) shows a broadened RF spectrum characteristic of a chaotic dynamics situation. Figure 2(c) shows the RF spectrum signature of a limit cycle (Period 1, P1) dynamics; with a strong peak at 3.8 GHz, frequency at which the VCSEL output oscillates. Figure 2(d) shows an RF spectrum indicating period doubling dynamics (Period 2, P2). Finally, Fig. 2(e) shows again a limit cycle (Period 1, P1) dynamics situation.

3.2 Orthogonal polarized optical injection

Figure 3(a) shows the experimental stability map of the 1550nm-VCSEL subject to orthogonally polarized optical injection into the subsidiary orthogonal polarization mode of the device. A bias current of 4 mA ($I_{Bias} = 2.44 \times I_{th}$) was applied to the VCSEL. The nonlinear dynamics have been mapped when the frequency of the externally injected signal is swept around the frequency of the orthogonal polarization of the fundamental transverse mode, f_{\perp} , the frequency detuning being $\Delta f = f - f_{\perp}$. Different regions corresponding to different dynamical regimes appear in the stability map. Region SIL represents the stable injection locking range, while region P1 show periodic dynamics (limit cycle or Period 1) and finally region CH corresponds to irregular and possibly chaotic dynamics. The SIL region exhibits

now an almost symmetric shape [21]. We believe that this could be perhaps related to the significant difference in the power emitted by the two orthogonal polarizations of the solitary VCSEL. The ratio of injected power to power emitted by the mode under injection would be much higher now than in the case of parallel polarized injection. Hence, the asymmetry of the Hopf bifurcation [23] [24] is not observed and an almost symmetric behaviour is found for the SIL region. Other factors that could be behind this behaviour would include the gain anisotropy and the large frequency splitting between the two orthogonal polarizations of the fundamental mode of the VCSEL. Additionally, Fig. 3(a) also shows the optical power required to obtain Polarization Switching (PS) [11–14]. PS refers to the situation where the output is switched from parallel to orthogonal polarization under orthogonally polarized optical injection [8–14]. This can be better understood with Figs. 3(b) and 3(c), which show respectively the optical spectrum of the free-running VCSEL (Fig. 3(b)) lasing in the parallel polarized mode, and the optical spectrum of the device subject to orthogonal optical injection (Fig. 3(c)) with an input power of $52 \mu\text{W}$ and frequency detuning of -0.9 GHz . In Fig. 3(c) the parallel polarized mode is suppressed, PS is attained and the output of the device changes to orthogonal polarization. It is found that PS is always accompanied with stable locking for negative frequency detuning (see Fig. 3(a)). However, PS can be also observed together with a periodic dynamical regime for certain values of positive frequency detuning, in particular with Period 1 dynamics (limit cycle) as shown in Fig. 3(a). The latter had only been reported previously in short-wavelength VCSELs [19], but had not been observed in long-wavelength devices.

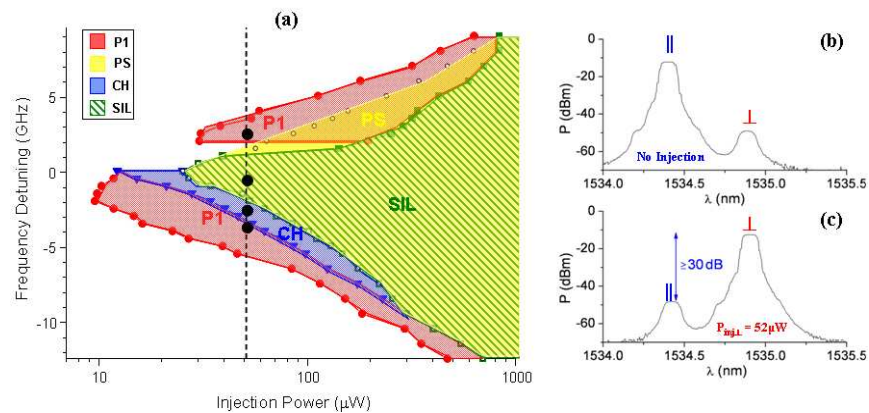


Fig. 3. (a) Stability map of the 1550nm-VCSEL subject to orthogonal injection. Different regions are observed: SIL (stable injection locking), PS (polarization switching), P1 (period 1) and CH (chaos); The black dots included in the map mark the nonlinear dynamic situations analyzed in Figs. 4(a-h). (b) Optical spectrum of the free-running VCSEL. (c) Optical spectrum of the VCSEL subject to orthogonal injection with input power of $52 \mu\text{W}$ and $\Delta f = -0.9 \text{ GHz}$. Polarization switching is produced. Applied bias current of 4 mA ($I_{\text{Bias}} = 2.44 \times I_{\text{th}}$) in all cases..

Figure 4 shows experimental RF spectra and time series measured for different dynamical regimes corresponding to the situations indicated by dots in Fig. 3(a). A fixed optical power of $52 \mu\text{W}$ was injected and different values of the detuning were considered. Figures 4(a) and 4(b) show a limit cycle dynamics (Period 1) situation appearing at positive frequency detuning where the RF spectrum of the device exhibits a high peak at 4.1 GHz which in the time domain results in strong periodic oscillations at that frequency. In region SIL, the orthogonal polarization mode of the VCSEL is stably locked to the ML and the output of the device exhibits a flat RF spectrum (except from a small lump corresponding to the relaxation oscillation frequency) and a flat time series, indicating CW operation (see Figs. 4(c) and 4(d) respectively). The shape of the SIL region is clearly different from that reported in a 845nm -VCSEL [19]. In our case the SIL region is symmetric around $\Delta f = 0$. However in previous

studies [19] injection locking at low input power appeared only at negative Δf . In 845nm-VCSELs injection locking only appears at positive Δf when the input power is high enough to excite the first-order transverse mode [19]. The CH region is characterized by a broadened electrical spectrum (Fig. 4(e)). The shape of these irregular dynamics in the time domain can also be seen in Fig. 4(f). In contrast with the results reported in [19], the irregular behaviour is only obtained for negative values of the frequency detuning and is not the result of a period doubling route to chaos. Finally, Fig. 4(g) shows the RF spectrum measured in the P1 region appearing at negative frequency detunings. In that situation the RF spectrum shows a major peak at approximately 1.8 GHz and several harmonics appearing at multiple values of that frequency. Finally, the time series (see Fig. 4(h)) shows that the output of the VCSEL oscillates periodically with a frequency of 1.8 GHz.

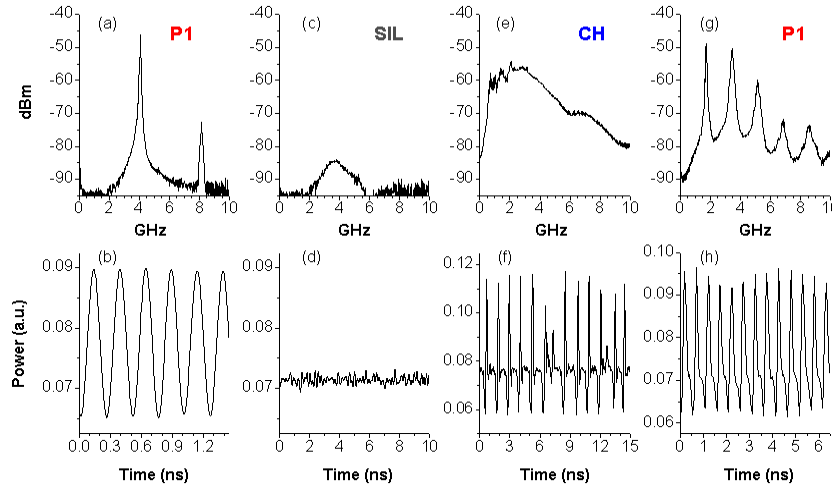


Fig. 4. Experimental RF spectra (a-d) and time series (e-h) measured when the 1550nm VCSEL is subject to orthogonal optical injection with a constant power of 52 μ W and for various cases of frequency detuning. (a,b) $\Delta f = 2.35$ GHz, (P1, period 1) (c,d) $\Delta f = -0.9$ GHz, (SIL, stable injection locking) (e,f) $\Delta f = -2.8$ GHz (CH, chaos) and (g,h) $\Delta f = -3.3$ GHz (P1, period 1).

4. Conclusions

We report a first experimental study of the nonlinear dynamics of a 1550 nm single transverse mode VCSEL with a preferred polarization. We report, for the first time to our knowledge, the experimental stability maps of this device subject to parallel and orthogonal optical injection. We have identified boundaries between regions of different behaviour, including periodic dynamics (limit cycle and period doubling), chaos and polarization switching. For the case of parallel polarized injection the results exhibit strong similarities with those previously reported in edge-emitting devices. However, a different stability map with new qualitative features was measured when the VCSEL was subject to orthogonal injection into the orthogonal polarization mode of the device. We also report for the first time the RF spectrum and time domain experimental signatures of the rich variety of nonlinear dynamics observed for the 1550nm-VCSEL subject to different polarized optical injection.

Acknowledgements

This work has been funded in part by the European Commission under the Programme FP7 Marie Curie Intra-European Fellowships Grant PIEF-GA-2008-219682 and by the Ministerio de Ciencia e Innovación, Spain, Project TEC2009-14581-C02-02.